Published in final edited form as:
Biochemistry. 1999 January 5; 38(1): 329–336. doi:10.1021/bi981964u.

Identification of a Site Critical for Kinase Regulation on the Central Processing Unit (CPU) Helix of the Aspartate Receptor†

Matthew A. Trammell and **Joseph J. Falke***
Department of Chemistry and Biochemistry, University of Colorado, Boulder, Colorado 80309-0215

Abstract

Ligand binding to the homodimeric aspartate receptor of *Escherichia coli* and *Salmonella typhimurium* generates a transmembrane signal that regulates the activity of a cytoplasmic histidine kinase, thereby controlling cellular chemotaxis. This receptor also senses intracellular pH and ambient temperature and is covalently modified by an adaptation system. A specific helix in the cytoplasmic domain of the receptor, helix α6, has been previously implicated in the processing of these multiple input signals. While the solvent-exposed face of helix α6 possesses adaptive methylation sites known to play a role in kinase regulation, the functional significance of its buried face is less clear. This buried region lies at the subunit interface where helix α6 packs against its symmetric partner, helix α6′. To test the role of the helix α6–helix α6′ interface in kinase regulation, the present study introduces a series of 13 side-chain substitutions at the Gly 278 position on the buried face of helix α6. The substitutions are observed to dramatically alter receptor function in vivo and in vitro, yielding effects ranging from kinase superactivation (11 examples) to complete kinase inhibition (one example). Moreover, four hydrophobic, branched side chains (Val, Ile, Phe, and Trp) lock the kinase in the superactivated state regardless of whether the receptor is occupied by ligand. The observation that most side-chain substitutions at position 278 yield kinase superactivation, combined with evidence that such facile superactivation is rare at other receptor positions, identifies the buried Gly 278 residue as a regulatory hotspot where helix packing is tightly coupled to kinase regulation. Together, helix α6 and its packing interactions function as a simple central processing unit (CPU) that senses multiple input signals, integrates these signals, and transmits the output to the signaling subdomain where the histidine kinase is bound. Analogous CPU elements may be found in other receptors and signaling proteins.

The aspartate receptor is a cell surface chemoreceptor that initiates chemotaxis up gradients of the chemoattractant aspartate in *Escherichia coli*, *Salmonella typhimurium*, and related bacteria. This receptor, together with several closely related receptors that are specific for different ligands, regulates a cytoplasmic phosphorylation pathway that controls the swimming state of the flagellar motor (1–7). Most of the pathway components assemble to form a stable signaling complex that uses the receptor as a structural framework (8,9). The core of this signaling superstructure is a ternary complex comprised of the homodimeric receptor molecule, the homodimeric histidine kinase CheA, and two copies of the bridging protein CheW. A pair of response regulator proteins, CheY and CheB, competitively bind to the complex at a site on CheA where they are activated by phosphorylation (9–12). Subsequently, these phosphoproteins dissociate and diffuse to their respective sites of action: phospho-CheY docks to and regulates the flagellar swimming motor, while phospho-CheB enzymatically restores the receptor covalent adaptation sites to their unmodified state (13–15). The enzyme CheR, which modifies the adaptation sites via methyl esterification of their glutamate side chains,

†Support provided by NIH Grant 40731.

*Corresponding author: Tel 303-392-3503; Fax 303-492-5894; falke@colorado.edu.

also binds to the signaling complex at a site near the C-terminus of specific receptors (16–18). Overall, the multicomponent architecture of the receptor signaling complex ensures rapid signal transmission through the phosphorylation pathway and speeds the chemotactic response to changing environmental conditions (19). Homologous phosphorylation pathways, termed the two-component class, are ubiquitious in prokaryotes and are widely distributed in eukaryotes (2,7,20). Many of the design features displayed by these ancient receptor-regulated pathways are widespread in more modern receptor systems; for example, G protein-coupled receptors also exhibit conformational transmembrane information transfer, adaptation via covalent modification, and formation of a multiprotein signaling complex.

The structure and mechanism of the homodimeric aspartate receptor have been studied intensively. The N-terminal half of the receptor is well characterized, as illustrated schematically in Figure 1. The crystal structure of the periplasmic domain has revealed that each subunit forms a periplasmic four-helix bundle and that the subunit interface is dominated by the N-terminal helices (α1) of each bundle (21). The first and last helices of each bundle (α1/TM1 and α4/TM2, respectively) extend across the bilayer to the cytoplasm, yielding a transmembrane four-helix bundle in which the packing interactions have been defined by disulfide mapping studies (22–24). Aspartate binding to one of the two periplasmic ligand binding sites generates an asymmetric conformational change that displaces the signaling helix, α4/TM2, relative to the static subunit interface (23–26). Several independent lines of evidence suggest that this displacement translates the signaling helix down its long axis toward the cytoplasm, generating a piston-type movement (26–28). Additional evidence indicates that the structural and mechanistic basis of transmembrane signaling is conserved in the superfamily of receptors that regulate two-component signaling pathways (28–34).

Less is known about the structure and mechanism of the C-terminal half of the receptor, which forms an independent folding domain beyond the cytoplasmic end of the signaling helix. This cytoplasmic domain is known to be elongated and highly α-helical, but structural analysis has been impeded by its dynamic nature (35–37). Cysteine and disulfide scanning studies, together with an alignment of 56 homologous domains in prokaryotic taxis receptors, have revealed four conserved α-helical regions in the C-terminal half of the domain (38–43). Two of these helices, α5 and α6, have been localized to the subunit interface where they are proposed to form coiled-coil interactions with the symmetric α5′ and α6′ helices from the other subunit of the homodimer (38–43,64).

Helix α6 of the cytoplasmic domain is particularly interesting because it processes multiple input signals, including (i) the transmembrane signal from helix TM2, which is coupled to the N-terminal end of helix α6 via two structured linkers and intervening helix α5, and (ii) the adaptation signal generated by methyl esterification of the adaptive glutamates, three of which lie on the exposed surface of helix α6 (38–43,16). Recent evidence suggests that helix α6 also accepts inputs from (iii) intracellular proton levels and (iv) ambient temperature in receptor-mediated pH taxis and thermotaxis, respectively (44; I. Kawagishi, personal communication). Thus, helix α6 plays a key role in the sensing and integration of four distinct input signals. The functional importance of this helix is highlighted by genetic studies identifying numerous helix α6 mutations that dramatically alter receptor function in vivo (50,51).

A variety of evidence indicates that helix α6 also plays a role in kinase regulation. The helix location is appropriately situated for such a role since it lies immediately N-terminal to the signaling domain, the independent structural unit known to bind the histidine kinase CheA and the coupling protein CheW (41–43,45–48). In the simplest model, kinase-activating signals pass through helix α6 on their way to the signaling domain, which transmits the signals to the bound kinase (48). Removal of helix α6 from the isolated domain inhibits kinase activity in vitro (48). The surface-exposed face of helix α6 is directly linked to kinase regulation, since it

possesses three adaptive glutamate side chains where methyl esterification by an adaptation enzyme is known to stimulate histidine kinase activity (48,49). It is less clear, however, how much the buried face and packing interactions of the helix contribute to kinase modulation. Limited evidence that the buried face is coupled to kinase regulation was generated by a study that scanned engineered cysteine residues and disulfide bonds through the region (38). The results of these and other random mutagenesis studies suggest that certain buried regions of helix α6 may be linked to kinase activity (39,50,51), but this proposal has not yet been tested.

The present study directly tests the functional role of the buried face of helix α6. Altogether, a series of 13 different side-chain substitutions are introduced at the buried Gly 278 position. These substitutions are found to yield extreme effects on kinase activity, ranging from kinase superactivation to full inactivation. Moreover, several of the substitutions lock the receptor in the kinase-activating state regardless of the presence of ligand. These and other results establish Gly 278 as a regulatory hotspot in the modulation of kinase activity. It follows that the buried face of helix α6, together with its exposed face and the closely associated signaling domain, plays a direct role in kinase regulation. Overall, this helix and its packing interactions serve as an intramolecular central processing unit (CPU) that senses and interprets multiple input signals, yielding an integrated output signal that is sent to the kinase via the signaling domain.

EXPERIMENTAL PROCEDURES

Materials

Plasmid pSCF6 and its mutated variants were used to express the aspartate receptor in the appropriate *E. coli* strains. This previously described plasmid is a pBlue-script KS^- plasmid containing the *S. typhimurium* aspartate receptor gene under control of its native promoter (23). Receptors utilized in in vitro studies were expressed in *E. coli* strain RP3808 *[Δ(cheA–cheZ)DE2209 tsr-1 leuB6 his-4 eda-50 rpsLi36 [thi-1 Δ (gal-attl) DE99 ara-14 lacY1 mtl-1 xyl-5 tonA31 tsx-78]/mks/)*. Tests of receptor function in vivo were carried out in *E. coli* strain RP8611 *[Δ (tsr)DE7028 Δ (tar–tap)DE5201 zbd::Tn5 Δ (trg)DE100 leu B6 his-4 rpsL136 [thi-1 ara-14 lac Y1 mtl-1 xyl-5 tonA31 tsx-78]/CP362 of G. Hazelbauer via F. Dahlquist, pa/)*. Both strains were kindly provided by J. S. Parkinson, University of Utah (52). Strains and plasmids used to express the soluble chemotaxis components CheA and CheW (HB101/pMO4 and HB101/pME5, respectively) were graciously provided by Jeff Stock, Princeton University, while the strain and plasmid used to express CheY (RBB455/pRBB40) were kindly provided by Bob Bourret, University of North Carolina. Mutagenic oligos and sequencing primers were obtained from Gibco–BRL, and sequencing reagents were purchased from Epicenter Technologies. L-[2,3-^{3}H]Aspartic acid (1 mCi/mL) and [γ-^{32}P]ATP (10 mCi/mL) were purchased from Amersham. All other materials were reagent-grade and were purchased from commercial suppliers.

Site-Directed Mutagenesis

Site-directed mutagenesis of Gly 278 in the native receptor was carried out by oligonucleotide-directed, site-specific mutagenesis as described by Kunkel (53) with modifications specified by the MutaGene T7 phagemid mutagenesis kit from Bio-Rad. Codon changes were verified by dideoxy plasmid DNA sequencing using a PCR method and thermostable DNA polymerase from Epicenter Technologies.

In Vivo Analysis of Receptor Function

The ability of the engineered receptors to mediate aspartate-specific chemotaxis was determined by performing chemotaxis swarm plate assays, using the *E. coli* strain RP8611 deleted for the aspartate receptor and transformed with mutated versions of plasmid pSCF6 as previously described (38). To test whether mutations significantly altered the receptor copy

number, the level of accumulation in RP8611 membranes was examined for each mutant receptor by isolating membranes from cells grown in swarm plate medium lacking agar. A given mutant was expressed by inoculating a 500 mL culture with a 1/250 dilution of cells grown to mid-log phase at 37 °C, and growth was continued at 30 °C until membranes were isolated according to the standard procedure (see below). Membranes were analyzed for receptor content by SDS–PAGE (see below).

Isolation of Receptor-Containing Membranes

Mutant and wild-type forms of the aspartate receptor were expressed in membrane vesicles by published procedures (38,54). The fraction of total membrane protein comprising the aspartate receptor was quantitated by laser densitometry of SDS–PAGE-resolved membrane components with an UltroScan XL densitometer (Pharmacia) and gels containing 10% acrylamide and 0.05% bisacrylamide (38,55). The total protein concentration in the membrane samples was independently measured by the BCA assay (56) in which the color-developing reactions were allowed to proceed for 25 min in 0.1% SDS at 65 °C prior to absorbance measurements at 562 nm utilizing a SoftMax kinetic microplate reader (Molecular Devices). Each 500 mL culture yielded approximately 5 mg of total membrane protein, of which the aspartate receptor typically comprised between 5% and 10%.

In Vitro Analysis of Receptor-Coupled Kinase Regulation

Chemotaxis proteins CheW, CheA, and CheY were isolated and purified as previously described (38). The ability of the engineered receptors to activate (in the absence of L-aspartate) and downregulate (upon addition of L-aspartate) the histidine kinase CheA was determined by an established receptor-coupled phosphorylation assay (23,38,49) with slight modifications as follows. Purified chemotaxis components were combined with portions of the isolated receptor-containing membranes to yield final monomeric concentrations of 6 μM aspartate receptor, 2 μM CheW, 0.25 μM CheA, and 10 μM CheY in 50 mM Tris, pH 7.5, 50 mM KCl, and 5 mM $MgCl_2$. The mixtures were preincubated 30 min at 22 °C, either with or without 1 mM L-aspartate, to allow formation of the receptor signaling complex. Phosphotransfer was initiated by adding [γ-^{32}P]ATP (4000–8000 cpm/pmol) to a final concentration of 100 μM ATP, and reaction aliquots were quenched at 10 s with 2× Laemmli sample buffer containing 25 mM EDTA. Quenched reaction samples were resolved by SDS–PAGE (16% acrylamide, 0.5% bisacrylamide, and 22% urea) and the gels were dried immediately following electrophoresis and phosphorimaged to determine the concentration of phospho-CheY in each quenched reaction sample. The initial rate of phospho-CheY formation by each signaling complex was determined from the slope of phospho-CheY produced between 0 and 10 s (within the linear range of the phosphotransfer reaction, data not shown). This rate was normalized to that obtained for the wild-type receptor, yielding the reported relative CheY phosphorylation rate for a given mutant.

Aspartate Binding Assays

K_D values for L-aspartate binding to mutant receptors in isolated membranes were determined by the previously described centrifugation assay (24,57).

RESULTS

Strategy for Probing the Role of the Buried Face of Helix α6 in Receptor Function

To probe the role of the buried face of helix α6 in the regulation of CheA kinase activity, a series of amino acid substitutions were engineered at the buried Gly 278 position. This position was chosen because it is the only residue that has been identified as critical in all four published libraries of randomly generated functional mutations. Specifically, an engineered cysteine scan

of 189 transmembrane and cytoplasmic positions revealed that G278C is one of only three cysteine substitutions that superactivate the kinase to a level 3-fold higher than that observed for the apo wild-type receptor (Figure 3 below; [23],24,38,39,[41]; Bass and Falke, manuscript in preparation). Scanning disulfide studies of these same 189 positions further showed that the Cys 278–Cys 278′ disulfide bond is one of only four intersubunit disulfides that lock the receptor in the kinase-activating state regardless of whether ligand is bound (23,24,38,39,41; Bass, Winston, and Falke, manuscript in preparation). Random mutagenesis yielded the G278A substitution in a pool of second-site revertants to a transmembrane signaling defect (51), while the G278D substitution appeared in a random library of signal locking mutations in the closely related serine receptor (50). (The effects of the latter G278A and G278D mutations on kinase activity are not known.) Finally, glycine is found at position 278 in all nine chemoreceptors of *E. coli* and *S. typhimuruim* (42,43), indicating that its function is strongly conserved.

Such findings suggest that the buried Gly 278 may play an unusually critical role in receptor function. To further test this hypothesis and to probe its mechanistic basis, the present study compares the functional effects of 13 substitutions at position 278. These include nonpolar side chains of varying size (Ala, Cys, Val, Leu, Ile, Met, Phe, and Trp), uncharged polar side chains (Ser, Thr, and Asn) and charged side chains (Asp and Arg). Since the receptor is a homodimer (58), each substitution modifies both the 278 and 278′ positions on symmetric helices α6 and α6′, respectively, within the same oligomer. The effects of these substitutions on receptor function are determined both in the full chemotaxis pathway in vivo and in the reconstituted receptor-regulated phosphorylation pathway in vitro.

Construction and Initial Characterization of Mutant Receptors

The 13 substitutions at position 278 were generated by oligonucleotide-directed mutagenesis of plasmid pSCF6. Subsequently, the mutant receptors were overexpressed in two *E. coli* strains, RP8611 and RP3808, that lack the aspartate receptor (52). Strain RP8611 possesses the soluble components of the chemotaxis pathway and was used in in vivo studies of receptor function. Strain RP3808, by contrast, is deleted for the soluble pathway components and was used to generate a homogeneous population of receptors for in vitro studies, lacking posttranslational modifications of the adaptation sites. Previous findings have shown that certain substitutions can damage the receptor in ways that prevent its accumulation in membranes (38,39,41); however, in the present case all mutant receptors accumulated to membrane levels similar to that observed for the wild-type receptor in both RP8611 and RP3808. It follows that each of the mutant receptors is a stable, well-folded, membrane-imbedded protein.

Effect of Substitutions on Receptor Function in Vivo

To determine the effect of substitutions on receptor function in vivo, mutant receptors expressed in *E. coli* strain RP8611 lacking the aspartate receptor were tested for their ability to restore cellular chemotaxis toward aspartate in the swarm plate assay (59). Because minor receptor perturbations can be offset by receptor overexpression and by the compensatory nature of the receptor adaptation system, the swarm assay is utilized to detect only those substitutions that yield major perturbations of receptor function. Figure 2 shows that, of the 13 engineered receptors tested, eight (Ala, Ser, Cys, Thr, Asn, Met, Leu, and Arg) retained the ability to mediate aspartate-specific chemotaxis, exhibiting a swarm rate at least 40% that observed for the wild-type receptor in this system. Four of these signal-retaining substitutions (Ala, Ser, Asn, and Met) yielded swarm rates equal within error to that of of wild type, while one (Arg) significantly speeded chemotactic swarming and three (Cys, Thr, and Leu) slightly slowed swarming (Figure 2). The remaining five substitutions (Val, Ile, Phe, Trp, and Asp) dramatically inhibited the aspartate-specific swarming, yielding rates less than 10% that of wild type. All of the mutant receptors were present at similar levels in the membrane (see

above), indicating that the loss of function observed for the five highly inhibited receptors was due to perturbation of receptor structure or mechanism. To further probe the nature of these perturbations, the in vitro assay for receptor-coupled kinase regulation was employed.

Effect of Substitutions on Receptor-Mediated Kinase Regulation in Vitro

The receptor-coupled kinase assay monitors the rate of phosphotransfer from the reconstituted receptor–kinase ternary complex (receptor, CheW, and CheA) to the response regulator CheY (11,12,23). Isolated *E. coli* RP3808 membranes containing a given engineered receptor were combined with CheW, CheY, and limiting amounts of CheA. Subsequently, the initial rate of CheY phosphorylation was measured in the presence and absence of saturating L-aspartate. The conditions employed ensured that receptor-stimulated CheA autophosphorylation was the rate-limiting step in phospho-CheY formation. When the wild-type receptor is utilized in this system, the rate of phospho-CheY formation is downregulated 10^2–10^3-fold upon aspartate binding to the periplasmic domain of the receptor (11,12,23), generating a large dynamic range over which subtle signaling perturbations can be detected.

Figure 3 depicts the rates of phospho-CheY formation mediated by each of the engineered receptor–kinase complexes relative to the wild-type rate, in both the absence and presence of L-aspartate. A wide range of effects on kinase regulation was observed, indicating a 50-fold difference in the abilities of the 13 aporeceptors to stimulate CheA autophosphorylation in the absence of aspartate. Remarkably, 11 of the 13 mutant aporeceptors (Ala, Ser, Cys, Thr, Met, Val, Leu, Ile, Phe, Trp, and Arg) yielded phospho-CheY formation rates that were significantly faster than wild type, while one (Asn) retained the wild-type rate and one (Asp) was at least 5-fold slower. Thus, most substitutions at Gly 278 superactivate CheA autophosphorylation, providing further evidence that this position plays a key role in the stimulation of kinase activity.

Addition of aspartate to nine of the receptors reduced the phospho-CheY formation rate 3-fold or more (Ala, Ser, Cys, Thr, Asn, Asp, Met, Leu, and Arg), indicating that these modified receptors retained at least partial ability to bind aspartate and downregulate the kinase (Figure 3). Binding of aspartate to the wild-type receptor, however, reduced phospho-CheY formation to undetectable levels, while 10 of the mutant receptors (Asn, Cys, Thr, Met, Val, Leu, Ile, Phe, Trp, and Arg) exhibit significant rates of phospho-CheY formation even in the presence of 1 mM aspartate. It follows that these 10 substitutions partially or fully trap the receptor in its on state. This effect was most striking for the four receptors (Val, Ile, Phe, and Trp) wherein aspartate failed to generate any significant kinase inhibition, leading to their classification as fully locked-on receptors. Such permanent kinase activation was similar to that observed when the Cys substitution was oxidized to form the C278–C278′ inter-subunit disulfide bond, thereby locking the receptor–kinase complex in the on state regardless of whether attractant is bound (38; Figure 3).

The failure of five mutant receptors (Asp, Val, Ile, Phe, and Trp) to support chemotaxis in vivo is fully explained by the results of the receptor-coupled kinase assay. Incorporation of the aspartate side chain at position 278 blocks chemotaxis by inhibiting kinase activation in the apo state of the receptor, while the valine, isoleucine, phenylalanine, and tryptophan substitutions prevent kinase downregulation upon attractant binding. Noteably, even partial attractant-triggered inhibition of CheA activity was sufficient for chemotaxis in vivo, since six mutations (Cys, Asn, Thr, Met, Leu, and Arg) that yielded partial lock-on activity were functional in the chemotactic swarm assay (compare Figures 2 and 3).

Aspartate Binding Assays

In principle, the four hydrophobic mutations (Val, Ile, Phe, and Trp) that fully lock the receptor in its kinase-activating state could do so either by inhibiting aspartate binding or by uncoupling the aspartate binding site from kinase regulation. These possibilities were distinguished by direct measurement of aspartate binding by a centrifugation assay (57). Isolated membranes containing a given receptor were incubated with varying concentrations of radiolabeled aspartate, and then the membranes were pelleted by ultracentrifugation and the concentrations of aspartate in the supernatant and pellet were determined. The resulting data were used to generate aspartate-binding curves for the wild-type and mutant receptors, thereby enabling determination of the aspartate K_D via best-fit analysis (24). The observed K_D values listed in Table 1 revealed that the mutant receptors retained essentially wild-type affinity for aspartate and were fully saturated at the 1 mM aspartate concentration used in the receptor-coupled kinase assay. Thus the valine, isoleucine, phenylalanine, and tryptophan substitutions block downregulation of kinase activity by uncoupling the ligand binding event from kinase regulation, rather than by preventing ligand binding. Failure to observe significant effects of mutations in the cytoplasmic domain on aspartate binding to the periplasmic domain is consistent with previous observation that cytoplasmic perturbations, including the C278–C278′ disulfide bond, typically have little or no effect on aspartate binding to the isolated, membrane-bound receptor (38,60).

DISCUSSION

The present findings explain the appearance of Gly 278 in all four published random screens for functionally important residues (23,24,38,39,41,50,51) and directly establish the importance of Gly 278 as a regulatory hotspot in the control of kinase activity. Symmetric side-chain substitutions at the 278 and 278′ positions are observed to have extreme effects on kinase activation. In the aporecep-tor–kinase complex, 10 of the 13 symmetric side-chain substitutions tested are found to superactivate the kinase, while one abolishes kinase activity. Moreover, when chemoat-tractant aspartate binds to the receptor, 10 of the 13 substitutions prevent the normal downregulation of CheA autophosphorylation and thus are classified as full or partial lock-on mutations. The effects of Gly 278 substitutions are most evident in vitro, where receptor-mediated kinase regulation can be monitored directly. In the cellular chemotaxis assay, where receptor overexpression and the adaptation system can counteract moderate receptor defects, many of the mutations become invisible and only those that fully abolish either kinase activation or its regulation by attractant are found to yield nonfunctional receptors.

The extreme effects of the engineered side chains on kinase activity explain the previously observed phenotypes of mutations at position 278. The G278D mutation, originally discovered at the corresponding position in the serine receptor because it trapped cells in the smooth-swimming state (50), is observed here to block kinase activation and cellular chemotaxis. The loss of kinase activation explains both the smooth-swimming behavior observed for the mutant and its failure to chemotax. The G278A mutation was originally identified as a second-site reversion that restores signaling to a defective receptor possessing the A19K mutation in its TM1 helix (51); here this G278 mutation is found to enhance the gain of the active kinase. It is therefore likely that the G278A reversion restores kinase activity lost due to the A19K mutation. More generally, the other 12 A19K reversions mapping to helix α6 (38,51) may well, like G278A, enhance kinase activity. Finally, the C278–C278′ disulfide bond characterized here and in previous studies (38) yields the same effect on kinase activity as the full lock-on substitutions G278V, G278I, G278F, and G278W, suggesting that these different perturbations of kinase regulation involve a similar mechanism.

Since Gly 278 is located on the buried face of helix α6, its tight coupling to kinase activity provides further evidence that the buried face is a key kinase control element. This face packs

against the symmetric face of helix α6′ from the other subunit as schematically shown in Figure 4 (38,40), where the lock-on nature of the intersubunit C278–C278′ disulfide bond demonstrates that the α6–α6′ interaction is fully formed in the kinase-activating state of the receptor (38). The broad spatial range of the buried helix surface suggests that besides the α6–α6′ interaction an additional packing element may be present (38). Gly 278 is situated on the edge of the buried face and could, in principle, contact both α6 from the other subunit and the hypothetical additional element (Figure 4). Current models propose that the unidentified element is a helix (putative helix α9) containing the fourth adaptation site (2,42,43). If such an additional element is present, the side-chain substitutions examined here may perturb the packing between this element and helix α6, as well as the α6–α6′ interface. In short, all of the various packing interactions involving the buried face of helix α6 may contribute to kinase regulation.

The present results suggest a working model for the regulatory mechanism of helix α6. The packing interactions of the helix are proposed to be modulated by multiple external signals including the transmembrane conformational change, the modification states and charges of the adaptation sites on the exposed surface of the helix, and cytoplasmic pH and temperature signals that are transmitted to the helix (26,44,48). The packing rearrangements triggered by these signals are likely to be relatively subtle; for example, aspartate binding to the membrane-bound receptor is known to generate only minor solvent exposure changes at positions within the α6 region (38). Together the multiple signals are proposed to yield an integrated, average position of helix α6 relative to its packing partners, thereby tuning the signal sent to the kinase-binding domain. In this picture, the helix α6 packing interactions serve as a continuously variable rheostat that regulate kinase activity.

Gly 278 is conserved in all of the *E. coli* and *S. typhimurium* chemosensory receptors, most likely because it enables full downregulation of kinase activity upon attractant binding. Alanine and serine are nearly equivalent in this respect, but both yield some detectable kinase activity in the ligand-bound state in contrast to glycine, which yields no detectable phosphorylation (see Figure 3). Thus, while other side chains optimize the activity of the receptor on-state, glycine appears to be chosen because it ensures the most inactive off-state. How does Gly 278 stabilize the inactive state of the receptor? The glycine residue could weaken helix–helix packing interactions involving helix α6, a model that is supported by the observation that the C278–C278′ interhelix disulfide bond yields the opposite effect. In this model, substitutions for glycine strengthen the interhelix interaction by providing additional packing forces or by reducing the helix dynamics. Alternatively, the small volume of the glycine residue could allow the regulatory helices to pack together as closely as possible in the receptor off-state. In this model, larger side chains, especially branched ones, prevent full kinase inactivation because they spread the regulatory helices farther apart. Further studies are needed to resolve these possibilities.

In principle, the hypothesized signal-induced rearrangement of the packing interface between the two cytoplasmic domains could be translated directly into kinase modulation. CheA is stable as a monomer but is only active in its dimeric state (61), indicating that interactions between the kinase subunits are essential for autophosphorylation (in particular, the autophosphorylation reaction is trans). Thus, rearrangements of the receptor subunit interface that are transmitted to the kinase subunit interface could directly modulate the autophosphorylation rate (66). Such a model must also explain, however, the observation that receptor heterodimers possessing one full-length subunit and one subunit missing its cytoplasmic domain are functional in vivo (62,63). One explanation proposes that two heterodimers can associate to form a partially active tetramer, bridged either by their unpaired cytoplasmic domains or by a kinase dimer. Signaling through one of the heterodimers would

break the C_2 symmetry of the tetramer, thereby modulating the interaction between kinase subunits.

Overall, the available evidence indicates that helix α6 is a central component of the receptor CPU. It accepts multiple input signals and sends an integrated output signal to the adjacent signaling domain, where the receptor contacts the associated CheA kinase and CheW proteins. The buried face of helix α6 and its packing interactions are essential to kinase regulation, as are the methylation sites on its exposed face. Further studies are needed to ascertain the mechanisms by which helix α6 senses and integrates multiple signals, and how it interprets and integrates these signals into a unified output signal that modulates the chemotactic phosphorylation pathway.

References

1. Taylor BL, Zhulin IB. Mol Microbiol 1998;28:683–690. [PubMed: 9643537]
2. Falke JJ, Bass RB, Butler SL, Chervitz SA, Danielson MA. Annu Rev Cell Dev Biol 1997;13:457–512. [PubMed: 9442881]
3. Stock, JB.; Surette, MG. Escherichia coli and Salmonella typhimurium: Cellular and Molecular Biology. Neidhardt, FC., editor. American Society for Microbiology Press; Washington, DC: 1996. p. 1103-1129.
4. Stock AM, Mowbray SL. Curr Opin Struct Biol 1995;5:744–751. [PubMed: 8749361]
5. Blair DF. Annu Rev Microbiol 1995;49:489–522. [PubMed: 8561469]
6. Bray D, Bourret RB, Simon MI. Mol Biol Cell 1993;4:469–482. [PubMed: 8334303]
7. Parkinson JS. Cell 1993;73:857–871. [PubMed: 8098993]
8. Gegner JA, Graham DR, Roth AF, Dahlquist FW. Cell 1992;70:975–982. [PubMed: 1326408]
9. Schuster SC, Swanson RV, Alex LA, Bourret RB, Simon MI. Nature 1993;365:343–347. [PubMed: 8377825]
10. Li J, Swanson RV, Simon MI, Weis RM. Biochemistry 1995;34:14626–14636. [PubMed: 7578071]
11. Borkovich KA, Kaplan N, Hess JF, Simon MI. Proc Natl Acad Sci USA 1989;86:1208–1212. [PubMed: 2645576]
12. Ninfa EG, Stock AM, Mowbray SL, Stock JB. J Biol Chem 1991;266:9764–9770. [PubMed: 1851755]
13. Barak R, Eisenbach M. Biochemistry 1992;31:1821–1826. [PubMed: 1737035]
14. Kehry MR, Doak TG, Dahlquist FW. J Bacteriol 1985;163:983–990. [PubMed: 3897203]
15. Hess JF, Oosawa K, Kaplan N, Simon MI. Cell 1988;53:79–87. [PubMed: 3280143]
16. Terwilliger TC, Koshland DE Jr. J Biol Chem 1984;259:7719–7725. [PubMed: 6330075]
17. Wu JG, Li JY, Li GY, Long DG, Weis RM. Biochemistry 1996;35:4984–4993. [PubMed: 8664291]
18. Okumura H, Nishiyama SI, Sasaki A, Homma M, Kawagishi I. J Bacteriol 1998;180:1862–1868. [PubMed: 9537386]
19. Bray D. Annu Rev Biophys Biomol Struct 1998;27:59–75. [PubMed: 9646862]
20. Wurgler-Murphy SM, Saito H. Trends Biochem Sci 1997;22:172–176. [PubMed: 9175476]
21. Milburn MV, Prive GG, Milligan DL, Scott WG, Yeh J, Jancarik J, Koshland DE Jr, Kim SH. Science 1991;254:1342–1347. [PubMed: 1660187]
22. Pakula AA, Simon MI. Proc Natl Acad Sci USA 1992;89:4144–4148. [PubMed: 1315053]
23. Chervitz SA, Lin CM, Falke JJ. Biochemistry 1995;34:9722–9733. [PubMed: 7626643]
24. Chervitz SA, Falke JJ. J Biol Chem 1995;270:24043–24053. [PubMed: 7592603]
25. Danielson MA, Biemann HP, Koshland DE Jr, Falke JJ. Biochemistry 1994;33:6100–6109. [PubMed: 7910759]
26. Chervitz SA, Falke JJ. Proc Natl Acad Sci USA 1996;93:2545–2550. [PubMed: 8637911]
27. Ottemann KM, Thorgeirsson TE, Kolodziej AF, Shin YK, Koshland DE Jr. Biochemistry 1998;37:7062–7069. [PubMed: 9585515]
28. Hughson AG, Hazelbauer GL. Proc Natl Acad Sci USA 1996;93:11546. [PubMed: 8876172]

29. Hughson AG, Lee GF, Hazelbauer GL. Protein Sci 1997;6:315. [PubMed: 9041632]
30. Weerasuriya S, Schneider BM, Manson MD. J Bacteriol 1998;180:914–920. [PubMed: 9473047]
31. Baumgartner JW, Kim C, Brissette RE, Inouye M, Park C, Hazelbauer GL. J Bacteriol 1994;176:1157–1163. [PubMed: 8106326]
32. Tatsuno I, Lee L, Kawagishi I, Homma M, Imae Y. Mol Microbiol 1994;14:755–762. [PubMed: 7891561]
33. Utsumi R, Brissette RE, Rampersaud A, Forst SA, Oosawa K, Inouye M. Science 1989;245:1246–1249. [PubMed: 2476847]
34. Krikos A, Conley MP, Boyd A, Berg HC, Simon MI. Proc Natl Acad Sci USA 1985;82:1326–1330. [PubMed: 3883356]
35. Long DG, Weis RM. Biochemistry 1992;31:9904–9911. [PubMed: 1390772]
36. Mowbray SL, Foster DL, Koshland DE Jr. J Biol Chem 1985;260:11711–11718. [PubMed: 2995347]
37. Seeley SK, Weis RM, Thompson LK. Biochemistry 1996;35:5199–5206. [PubMed: 8611504]
38. Danielson MA, Bass RB, Falke JJ. J Biol Chem 1997;272:32878–32888. [PubMed: 9407066]
39. Butler SL, Falke JJ. Biochemistry 1998;37:10746–10756. [PubMed: 9692965]
40. Chen X, Koshland DE Jr. Biochemistry 1997;36:11858–11864. [PubMed: 9305978]
41. Bass RB, Falke JJ. J Biol Chem 1998;39:25006–25014. [PubMed: 9737956]
42. Danielson, MA. PhD Thesis. Department of Chemistry and Biochemistry, University of Colorado; Boulder, CO: 1997. The molecular mechanism of transmembrane signaling and kinase regulation by the aspartate receptor of bacterial chemotaxis.
43. Le Moual H, Koshland DE Jr. J Mol Biol 1996;261:568–585. [PubMed: 8794877]
44. Nishiyama SI, Nara T, Homma M, Imae Y, Kawagishi I. J Bacteriol 1997;179:6573–6580. [PubMed: 9352902]
45. Liu JD, Parkinson JS. J Bacteriol 1991;173:4941–4951. [PubMed: 1860813]
46. Ames P, Yu YA, Parkinson JS. Mol Microbiol 1996;19:737–746. [PubMed: 8820644]
47. Ames P, Parkinson JS. J Bacteriol 1994;176:6340–6348. [PubMed: 7929006]
48. Surette MG, Stock JB. J Biol Chem 1996;271:17966–17973. [PubMed: 8663397]
49. Borkovich KA, Alex LA, Simon MI. Proc Natl Acad Sci USA 1992;89:6756–6760. [PubMed: 1495964]
50. Ames P, Chen J, Parkinson JS. Cold Spring Harbor Symp Quant Biol 1988;53:59–66. [PubMed: 3076088]
51. Oosawa K, Simon MI. Proc Natl Acad Sci USA 1986;83:6930–6934. [PubMed: 3018752]
52. Liu JD, Parkinson JS. Proc Natl Acad Sci USA 1989;86:8703–8707. [PubMed: 2682657]
53. Kunkel TA, Bebenek K, McClary J. Methods Enzymol 1991;204:125–139. [PubMed: 1943776]
54. Foster DL, Mowbray SL, Jap BK, Koshland DE Jr. J Biol Chem 1985;260:11706–11710. [PubMed: 2995346]
55. Laemmli UK. Nature 1970;227:680–685. [PubMed: 5432063]
56. Stoscheck CM. Methods Enzymol 1990;182:50–68. [PubMed: 2314256]
57. Clarke S, Koshland DE Jr. J Biol Chem 1979;254:9695–9702. [PubMed: 385590]
58. Milligan DL, Koshland DE Jr. J Biol Chem 1988;263:6268–6275. [PubMed: 2834370]
59. Adler J. Science 1966;153:708–716. [PubMed: 4957395]
60. Iwama T, Homma M, Kawagishi I. J Biol Chem 1997;272:13810–13815. [PubMed: 9153237]
61. Surrette MG, Levit M, Liu Y, Lukat G, Ninfa EG, Ninfa A, Stock JB. J Biol Chem 1996;271:939–945. [PubMed: 8557708]
62. Tatsuno I, Homma M, Oosawa K, Kawagishi I. Science 1996;274:423–425. [PubMed: 8832891]
63. Gardina PJ, Manson MD. Science 1996;274:425–426. [PubMed: 8832892]
64. Singh M, Berger B, Kim PS, Berger JM, Cochran AG. Proc Natl Acad Sci USA 1998;95:2738–2743. [PubMed: 9501159]
65. Cochran AG, Kim PS. Science 1996;271:1113–1116. [PubMed: 8599087]
66. Stock J. Curr Biol 1996;6:825–827. [PubMed: 8835862]

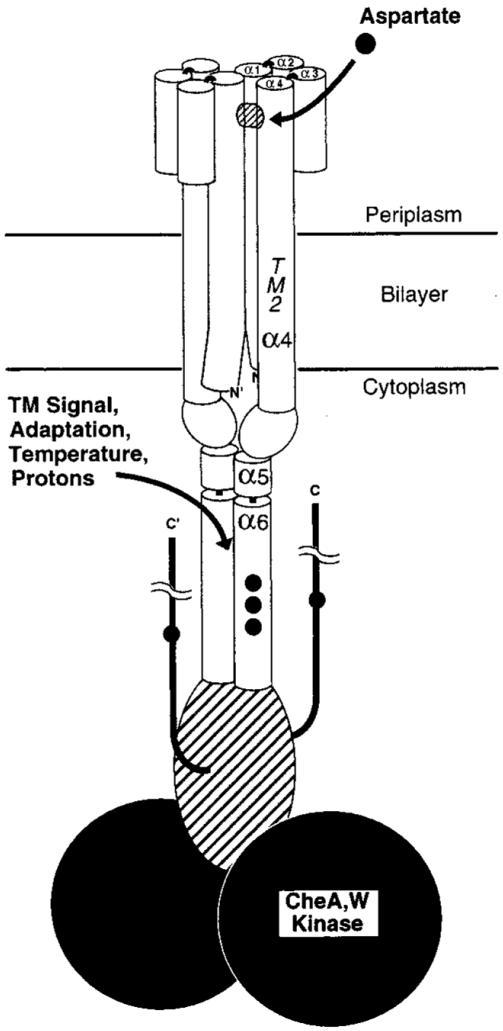

Figure 1.

Schematic model of the aspartate receptor. Shown are the well-characterized four-helix bundles that comprise the periplasmic and transmembrane regions of the homodimeric structure (21–24), as well as the current picture of the cytoplasmic domain wherein helices α4, α5, and α6 have been experimentally detected (38–40). The latter two helices are located at the subunit interface where they pack against their symmetric partners. [A fourth helix detected recently in the signaling domain, helix α7, is omitted for simplicity (41).] To distinguish the two subunits, the helices are labeled on only one of them. Each subunit possesses four adaptive methylation sites, shown as small solid circles (16). Helix α6 possesses three of the methylation sites, and its C-terminus is contiguous with the signaling domain (hatched) that binds the histidine kinase CheA and the coupling protein CheW (42,43,45–48). The fourth methylation site is located C-terminal to the signaling domain, in a region where the structure has not yet been experimentally defined.

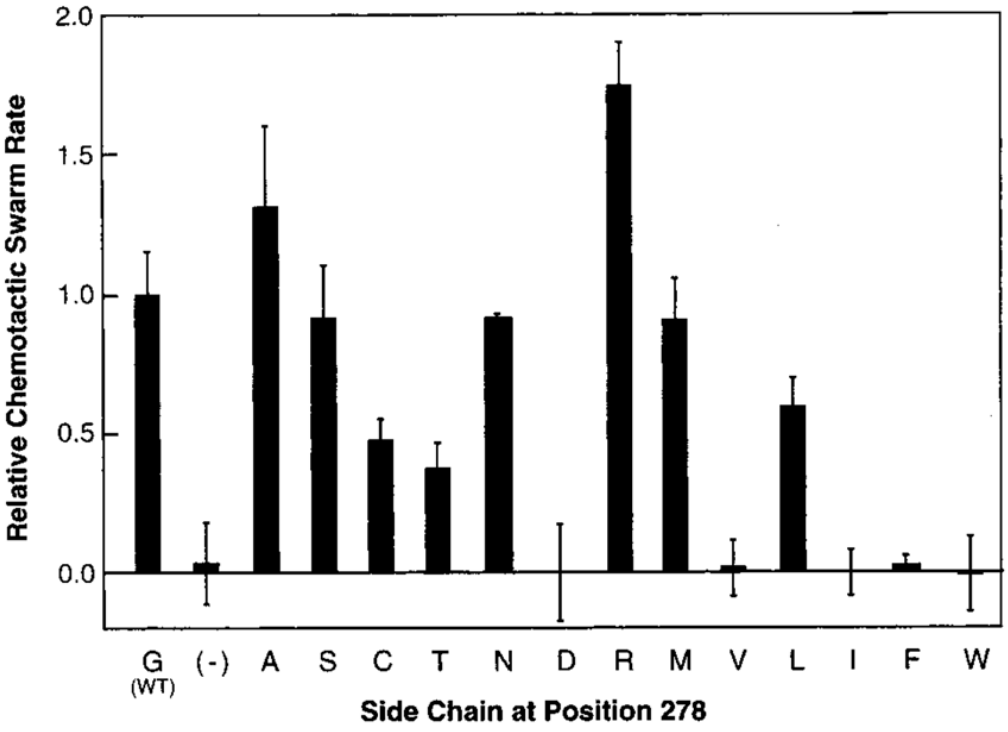

Figure 2.

Effects of side-chain substitutions at position Gly 278 on receptor-mediated chemotaxis in vivo. Receptors were expressed in an *E. coli* strain lacking the aspartate receptor and examined for their ability restore migration up a self-generated gradient of L-aspartate on chemotactic swarm plates at 30 °C. For each mutant receptor, the aspartate-specific component of chemotaxis was determined by the difference in swarm rates in the presence and absence of aspartate. Subsequently, this difference was normalized to the corresponding difference observed for the wild-type receptor expressed in the same system, yielding the indicated relative swarm rate. Error bars indicate one standard deviation ($n \geq 3$).

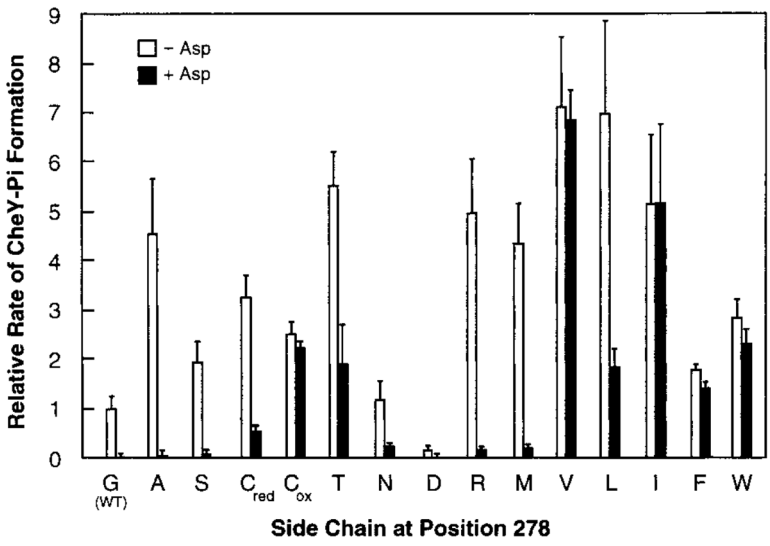

Figure 3.

Effects of side-chain substitutions at position Gly 278 on receptor-mediated kinase regulation in vitro. Isolated *E. coli* membranes containing the mutant receptor of interest were reconstituted with the CheA, CheW, and CheY molecules to yield an active receptor–kinase signaling complex. The vertical bars indicate the kinase activities observed for the mutant signaling complexes relative to that of the wild-type complex, both in the absence (open bars) and presence (solid bars) of bound aspartate at 25 °C. The measured parameter, the phospho-CheY formation rate, is proportional to the limiting rate in the phosphorylation pathway, namely, the rate of receptor-regulated CheA autophosphorylation. To facilitate comparison with the point mutations, the effect of the engineered C278–C278′ disulfide bond on kinase activity was redetermined as previously described (38). Error bars indicate one standard deviation ($n \geq 3$).

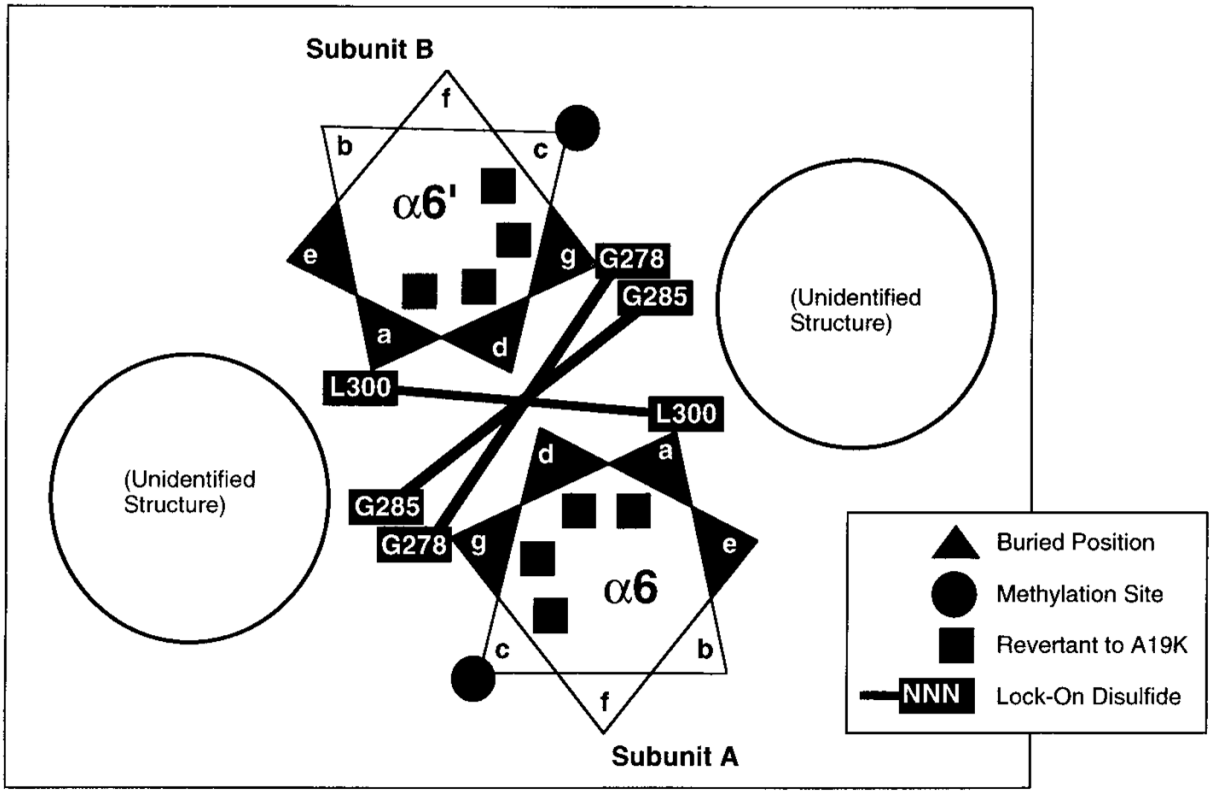

Figure 4.

Schematic helical wheel model for the packing of helices α6 and α6′ at the subunit interface, based on prior cysteine and disulfide scanning studies of positions 265–309 (for additional details see ref 38). The view is down the helix axes, looking from the membrane toward the cytoplasm. Each helix is shown as a repeating heptad where the a and d positions are highly hydrophobic, as expected for a coiled-coil or four-helix bundle interaction. The positions of disulfide bonds that lock the receptor in the kinase-activating state are indicated (connected, solid rectangles), as are the buried positions defined by solvent exposure measurements (solid triangles) (38). A series of second-site reversions known to restore signaling to a receptor possessing a defective transmembrane signaling domain (A19K) map to this same buried packing surface (solid squares) (51). The solvent-exposed adaptive methylation sites are located at the c position on the exposed face (solid circles), as are the remaining second-site reversions. The broad extent of the buried face suggests the presence of two additional, unidentified structural elements that pack against the α6 and α6′ helices, as indicated by the large circles (38).

Table 1

Effects of G278 Substitutions on Aspartate Affinity

receptor	Asp K_D[a] (μM)	affinity relative to WT
G278 (WT)	2.1 ± 0.5	1.0
G278L	4.0 ± 2.0	0.5
G278V	1.2 ± 0.4	1.8
G278I	2.5 ± 2.1	0.8
G278W	2.2 ± 0.9	1.0
G278F	1.0 ± 0.2	2.1
G278T	3.5 ± 0.9	1.7
G278D	4.8 ± 3.5	0.4

[a] Indicated is the mean and standard deviation ($n \geq 3$).